

Optimal diffusion-gradient waveforms for measuring axon diameter

I. Drobnjak¹, B. Siow², and D. C. Alexander¹

¹Center for Medical Image Computing, Department of Computer Science, University College London, London, London, United Kingdom, ²Center for Advanced Biomedical Imaging, University College London, London, United Kingdom

Introduction: Measuring microstructure parameters of brain tissue, such as axon radius, in vivo is a challenge in diffusion MRI. Current approaches typically use pulsed-gradient spin-echo (PGSE) [1] or stimulated-echo (STEAM) [2] sequences, both of which use a rectangular diffusion-gradient pulse. However other shapes of diffusion-gradient pulses such as oscillating [3] or chirped [4] may provide more sensitivity to microstructure features, particularly at low gradient strengths available on clinical scanners. Here, we optimize the shape of the diffusion-gradient waveform, constrained only by hardware limits and to have fixed orientation, to give the best estimate of axon radius based on a simple model of the diffusion within white matter.

Methods: We adapt the optimisation framework described in [1], which finds pulse sequence combinations that minimize the Cramer-Rao Lower Bound (CRLB) on parameters of a model to fit to a set of measurements. The pulse sequence has the form of a PGSE sequence, as shown in figure 1. The gradient-pulse waveforms are each defined by N equally spaced points constrained only so that the maximum gradient strength is $|G|=0.045T/m$ and the slew rate does not exceed $225T/m/s$. The first and the last point of the waveform are constrained to zero. The N points define the first gradient pulse, prior to the 180-degree pulse and the second gradient pulse is constrained to be the mirror reflection of the first. The tissue model is as described in [1] (composition of hindered and restricted diffusion compartments [11] with a single axon radius). For the arbitrary diffusion-gradient waveforms we compute the restricted compartment signal using the matrix formalism [5], and the hindered compartment signal using the Stejskal and Tanner equation [6]. The optimized protocols contain four different measurements [1], each with a gradient direction orthogonal to the axon direction, resulting in $4 \times (N-2)$ parameters to optimize. We fix the echo time $TE=80ms$ and set $N=53$. A-priori model parameters for the optimization were: volume fraction $f=0.7$, intrinsic diffusivity $d_{||}=1.7 \times 10^{-9} m^2 s^{-1}$ and apparent diffusion coefficient $d_{\perp}=1.2 \times 10^{-9} m^2 s^{-1}$; we run separate optimizations for axon radii $R=0.5, 1, 2, 3, 5 \mu m$.

The optimized protocol was evaluated against the optimized PGSE sequence [1] by: a) comparing the value of respective objective functions; b) comparing the accuracy of estimating R. The latter was done according to [1]: Each optimized protocol was used to calculate synthetic data and find the posterior distribution on R, which we sample using MCMC.

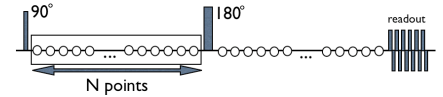


Fig1. General-gradient (GEN) sequence.

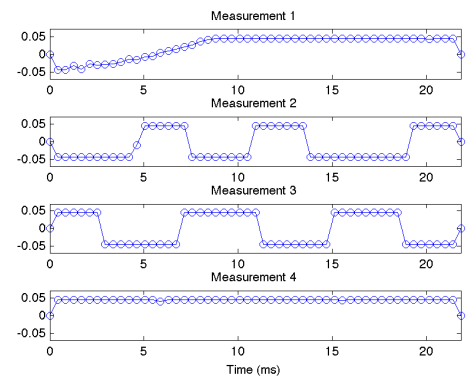


Fig2. Optimized gradient waveforms, $R=3 \mu m$.

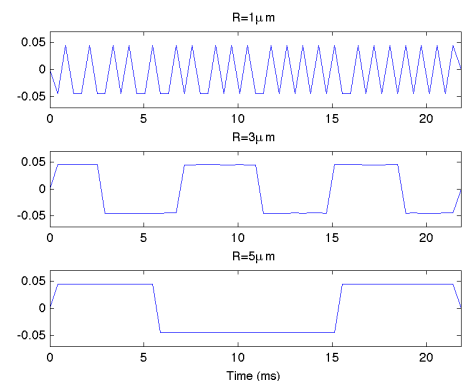


Fig3. Oscillating waveform with the highest frequency for each optimized protocol, $R=1, 3, 5 \mu m$.

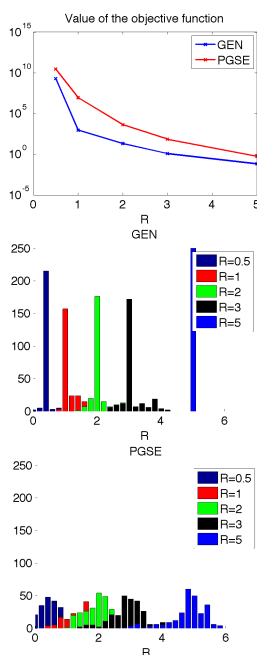


Fig4. Comparison between GEN and PGSE. Top: Cost function. Bottom two: Posterior distribution on radius R for each true R.

Results Figure 2 shows the optimized protocol for $R=3 \mu m$. Observe that only one of the measurements (4) contains one PGSE-like rectangular pulse while the other three are distinctly different from PGSE. In particular, two measurements (2,3) have oscillating square waveform, a pattern we consistently observe in the optimized protocols. Furthermore, the frequency of these oscillating waveforms is inversely proportional to the a-priori setting of R as seen in figure 3. Figure 4 shows the value of cost function for GEN and PGSE sequences as a function of radius R. We consistently obtain lower values of the objective function for the GEN gradient waveforms compared to PGSE protocols, which suggests better sensitivity. Moreover, as can be seen in the middle (GEN) and the bottom (PGSE) row of figure 4, the posterior distributions on R are markedly narrower for the generalized waveforms, demonstrating high precision in estimating the radius, substantially more than the optimized standard PGSE.

Discussion: Our optimization of the arbitrarily shaped diffusion-gradient waveform, (subject only to hardware limits and fixed orientation), suggests that square-wave oscillating gradients maximize sensitivity to pore size over the set of PGSE sequences. They also show that the frequency of the waves increases as the radius size decreases. The results support previous work eg [3] that models the signal from sinusoid oscillating gradient pulses and shows that higher frequency corresponds to a smaller effective diffusion time, which provides sensitivity to smaller pore sizes. Each period of the oscillation is similar to a separate PGSE experiment with diffusion time similar to the period; multiple periods emphasise sensitivity to displacements over that diffusion time. The square-wave arises because it maximizes the diffusion weighting in each period. There is scope for further development of the optimization. First, here we fix the echo time for the arbitrary waveforms, but could extend the idea so that the optimization chooses it directly as it does for the PGSE optimization in [1]. Second,

here we limit the technique to optimize sequences with the same structure as the standard PGSE sequence with fixed gradient orientation. The method itself can be extended easily to allow the gradient orientation to vary arbitrarily. We can also extend to more complex sequence types so that the search space includes dual spin-echo [7], double wave vector [8], multi-pulse PGSE [9], spinning gradient [10] sequences. All these extensions increase the dimension of the search space, but this very general optimization can be used to identify the broad class of protocols, which we can then parametrize to perform more targeted optimizations. For example, we might constrain each measurement of the protocol to have square wave pulses and optimize just the amplitude, frequency and duration. The main direction of the future work is validation using realistic scanner measurements, which is straightforward, since we purposefully constrain the optimization to produce realizable waveforms; [3] note that high frequency gradient oscillations are readily achievable on standard MRI scanners.

References: [1]Alexander MRM08 [2]Avram JMR04 [3]Xu MRM09 [4]Kiruluta ISMRM08 [5]Codd JMR99 [6]Price CMR97 [7]Clayden IPMI09 [8]Komlos MRM08 [9]Ozarlan JMR07 [10] Van Wedeen ISMRM08 [11] Assaf MRM08